



**HAL**  
open science

# Realization and preliminary tests of an axial-flux synchronous machine with HTS armature windings

Hocine Menana, Yazid Statra, Bruno Douine

► **To cite this version:**

Hocine Menana, Yazid Statra, Bruno Douine. Realization and preliminary tests of an axial-flux synchronous machine with HTS armature windings. Symposium on Advanced Technologies in Electrical Systems - SATES23, Mar 2023, Arras, France. hal-04165301

**HAL Id: hal-04165301**

**<https://hal.science/hal-04165301>**

Submitted on 18 Jul 2023

**HAL** is a multi-disciplinary open access archive for the deposit and dissemination of scientific research documents, whether they are published or not. The documents may come from teaching and research institutions in France or abroad, or from public or private research centers.

L'archive ouverte pluridisciplinaire **HAL**, est destinée au dépôt et à la diffusion de documents scientifiques de niveau recherche, publiés ou non, émanant des établissements d'enseignement et de recherche français ou étrangers, des laboratoires publics ou privés.



# Realization and preliminary tests of an axial-flux synchronous machine with HTS armature windings

**Hocine MENANA, Yazid STATRA and Bruno DOUINE**

Université de Lorraine, GREEN, F-54000 Nancy, France.

[name.surname@univ-lorraine.fr](mailto:name.surname@univ-lorraine.fr)

**Objective** – The aim of this work is to show the possibility to develop synchronous machines with armature windings made of high temperature superconductors (HTS). The construction and the preliminary tests of a handmade prototype of an axial field HTS synchronous are presented.

**Findings** – Several tests have been conducted at liquid nitrogen temperature. The measurements have been comforted by modeling results obtained by a 3D finite element model of the studied machine. Investigations on AC loss and their measurement for HTS coils mounted on iron part are also carried out. The preliminary tests on the prototype, in both modeling and measurements, are very promising.

**Originality** – The application of high temperature superconductors in electrical machines is mainly limited to inductors in synchronous machines, due to the AC losses which can be excessive. In this work, we show the possibility of their use as an armature, handling some precautions. The approach is based on the combined use of modeling and measurements.

**Keywords** – HTS armature winding, Axial-flux synchronous machine AC Losses, Modeling, Measurements.

## 1. Introduction

Superconducting machines are an important area of research related to applied superconductivity. The use of superconducting materials can provide performance in terms of power density better than that of conventional electrical machines. Indeed, such materials, in their wire configuration are able to carry high current densities with very low losses and to produce very large fields, while, in their massive form, they are able to screen strong fields or to trap inductions several Tesla higher than those of permanent magnets. These characteristics make it possible to envisage gains in the mass, size and efficiency of the machines, which are all the greater when the temperature is low. Targeted applications for superconducting machines range from ship propulsion to power generation. Nevertheless, the investment and operating costs represent a disadvantage that slows down their development on an industrial scale.

The integration of superconductors in electrical machines can be done in different ways. The most commonly encountered is based on the same structures as classical machines. Synchronous machines include the majority of machines produced, where the superconducting part concerns the inductor of the machine [1]. Among the superconducting machines produced, we can mention those of: the SIEMENS company with a power of 4 MVA at 3600 rpm based on the BSCCO [2] ribbon, of the AMERICAN SUPRACONDUCTORS which has a power of 36, 5 MW at 120 rpm [3], from CONVERTEAM with a power of 250 kW at 1500 rpm, designed in partnership with the GREEN Laboratory [4]. Recently, the EU-funded EcoSwing project successfully demonstrated the first superconducting HTC generator with an output of 3.6 MW at 15 rpm, mounted on a direct drive wind turbine. A 24% weight reduction compared to commercial permanent magnet generators is achieved in this first, not fully optimized prototype. For an optimized generator the power can reach 6 MW and the weight reduction should be around 40% [5-7].

Machines, with original inductor structures, use HTS in a massive form (bulks) as superconducting magnets as a substitute for permanent magnets [8], or as superconducting screens to obtain a certain spatial modulation of the magnetic field. In this last category, the GREEN laboratory has studied, produced and tested various machines based on the principles of flux modulation [9-11] or flux deviation [4, 12], with a combined use of superconducting wires and massive superconductors.

Fully superconducting machines use superconducting materials for both the armature and the inductor. This type of machine has more advantages, such as increasing the current density of the armature, reducing Joule effect losses and decreasing the thickness of the air gap (the cryostat enclosing the whole machine), which make it possible to achieve higher power densities and efficiencies. However, AC losses are still a significant brake on their development, even

though the feasibility and efficiency has been proven through various prototypes: totally superconducting [13-14], or permanent magnet and induced superconducting [15-18]. 2G SHTCs based on twisted filaments and MgB2 yarns seem to be potential candidates for such structures [1, 19].

In this work, we present the implementation and the tests of a prototype of an axial flux synchronous machine with a superconducting armature. The structure of the prototype is made by recycling a superconducting axial flux coupling prototype made and tested in previous works [20-21]. An integral modeling approach has been developed to determine the critical current of the coils, not to be exceeded during operation, and the various global quantities characterizing the machine. We describe the various measurements on the prototype and the results obtained by both modeling and measurements.

## 2. The structure of the prototype

The prototype, with an external diameter of approximately 30 cm, is composed of a permanent magnet rotor and a stator carrying three-phase superconducting windings cooled with liquid nitrogen (Fig.1).

The rotor consists of four permanent NdFeB type cylindrical magnets mounted on a ferromagnetic yoke at the middle radius, forming four (4) magnetic poles ( $p=2$ ). The cylindrical yoke in E24 mild steel, is sized to avoid magnetic saturation.

The superconducting armature illustrated is made up of three superconducting coils arranged on a ferromagnetic yoke, at the middle radius, in the air gap (absence of ferromagnetic notches). The *FeSi* ferromagnetic yoke is laminated in the radial direction to limit eddy current losses.

The specifications of the different parameters are given in Table 1 [22].

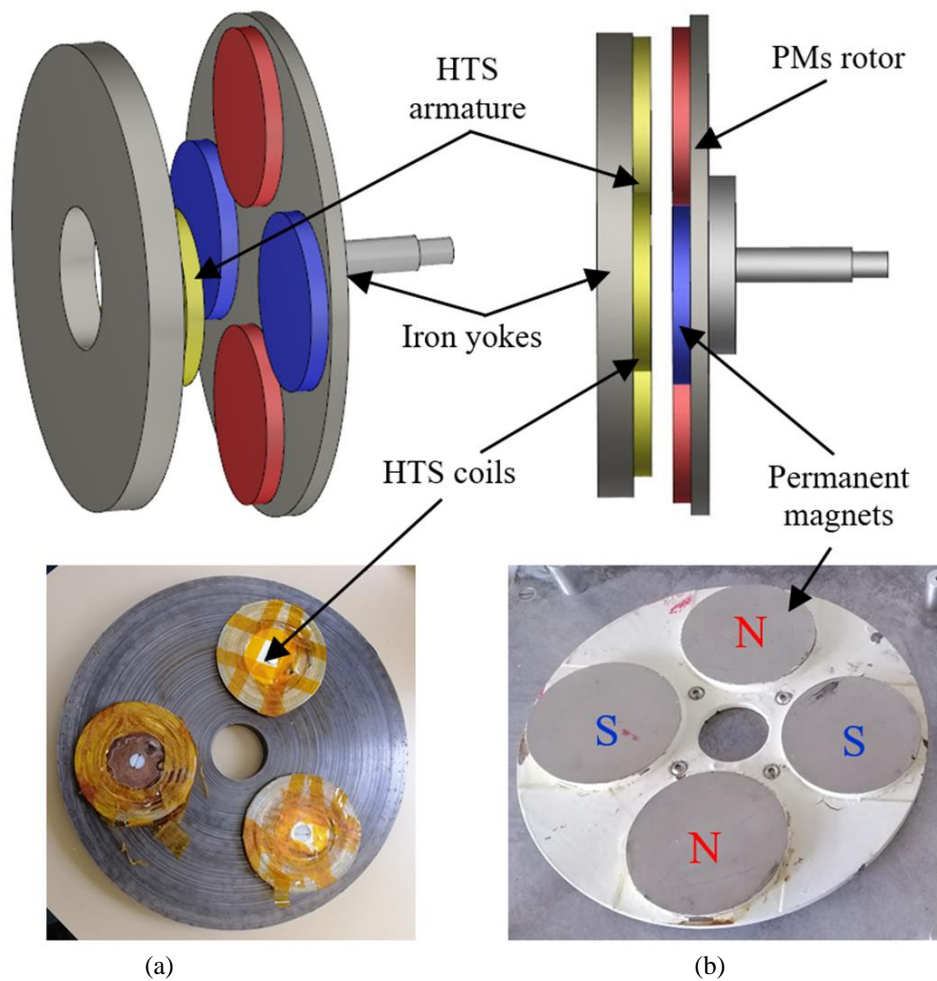


Figure 1 : The stator and rotor of the realized HTS synchronous machine prototype: (a) rotor, (b) stator

Table 1. Parameters specifications []

	Parameter	Value
HTS coil (insulated layer)	Tape measured critical current at 77K (self-field)	69.5 A
	Average of the measured coils critical currents at 77K (self-field)	43.3 A
	Number of turns	63
	Inner radius	25 mm
	Outer radius	50 mm
	Thickness	3.1 mm
	Total wire length ( $L_c$ )	14.8 m
NdFeB magnet (disc type)	Remanence	1.25 T
	Thickness	10 mm
	Radius	50 mm
HTS armature	Iron yoke thickness	20 mm
	Iron yoke Inner radius	25 mm
	Iron yoke Outer radius	152 mm
	Number of coils	3
PM rotor	Iron yoke thickness	10 mm
	Iron yoke Inner radius	25 mm
	Iron yoke Outer radius	140 mm
	Number of PMs	4
HTS-AFSM	Airgap (e)	10 mm
	Number of pole pairs	2
	Mean radius	85 mm

### 3. Experimental characterization

Electric methods are used to characterize the HTS coils, separately and in their integration in the machine. The electric model  $E(J)$  and the critical current ( $J_c$ ) of the superconductor are characterized in DC using a direct current source and a nanovoltmeter, as presented in Figure 2. The element is supplied by a direct current  $I$ , and the potential difference  $U$  across its terminals is measured. The critical electric field ( $E_c$ ) is set to  $1\mu\text{V}/\text{cm}$ . The critical voltage ( $U_c$ ) of the sample is the product of the critical electric field with the length between the points of the potential measurement ( $L$ ) and the critical current ( $I_c = J_c \times S$ ), where  $S$  is the tested sample section, is the current giving the critical voltage. The  $E(J)$  dependency is generally expressed by the power law given by Eq. (1), where  $n$  is the creep exponent.

$$U = U_c \left( \frac{I}{I_c(B)} \right)^n \Rightarrow E = E_c \left( \frac{J}{J_c(B)} \right)^n$$

$$U = E \times L$$

$$I = J \times S$$
(1)

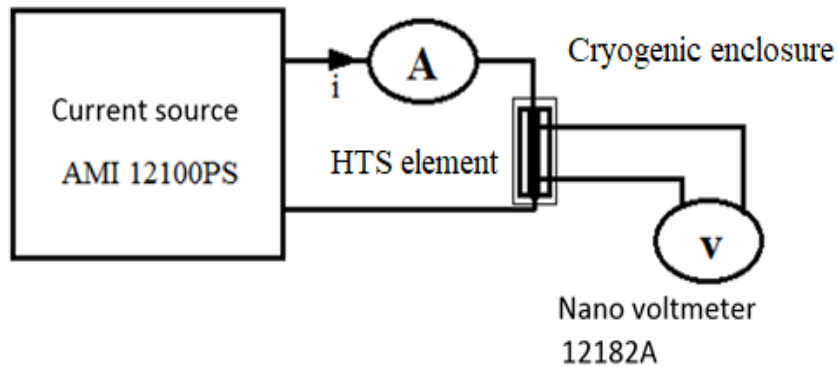


Figure 2: DC characterization of HTS coils

Figure 3 shows the test bench for the measurement of AC losses using a synchronous detection. The superconductive element is supplied by a sinusoidal AC current source. An isolation transformer is used to avoid electromagnetic disturbances passing through the mass. The voltage measured across the element contains a resistive part which is in phase with the current and responsible for the losses, and an inductive part which is a few hundred times higher than the resistive part which is of interest. The inductive part is thus compensated using a compensation coil connected in series with the measurement wires, and positioned near the power supplying cable. The compensation coil orientation is chosen so that the mutual inductance ( $M$ ) with the supplying cable is in opposition with the inductance ( $L$ ) of the tested element. The measured voltage is then given as follows [23]:

$$U(t) = U_{\text{losses}}(t) + (L - M) \frac{di(t)}{dt} \quad (2)$$

The measured voltage is non-sinusoidal due to the non-linear behavior of the superconductor. The AC losses are only related to the fundamental of this voltage, given by Eq. (3), where,  $I_{\text{rms}}$ ,  $U_{1\text{rms}}$ , and  $\varphi_1$  denote respectively the RMS of the current, the RMS of fundamental of the voltage signal, and the phase shift between them. If the applied current is not sinusoidal, a numerical integration in an oscilloscope is used to evaluate the losses

$$P = I_{\text{rms}} U_{1\text{rms}} \cos(\varphi_1) \quad (3)$$

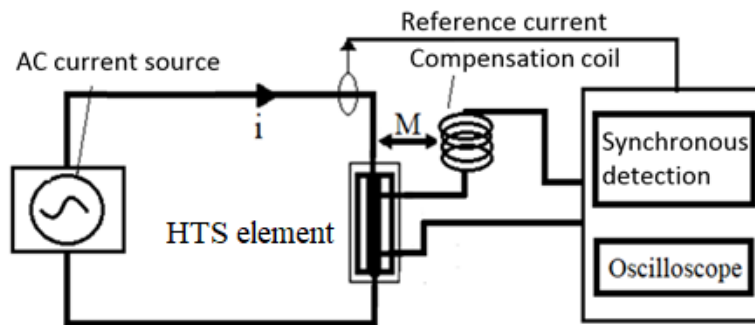


Figure 3. The AC losses measurement system.

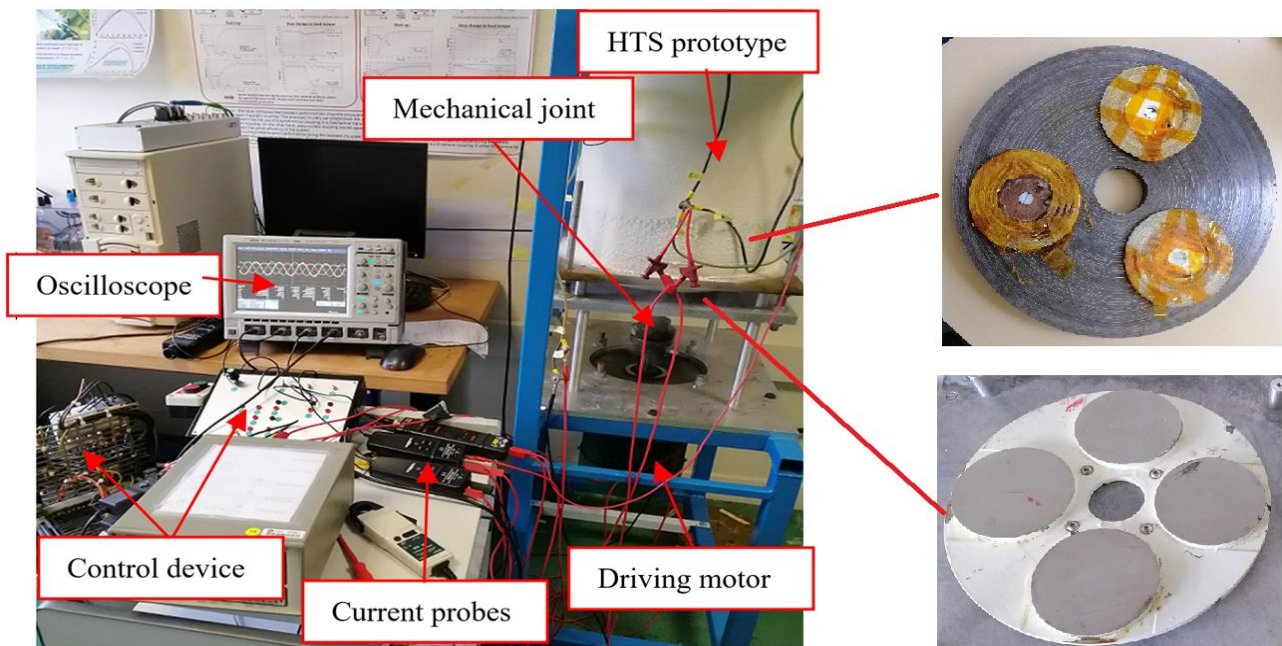


Figure 4. The test bench

The test bench for the prototype characterization and tests is shown in Figure 4. The machine is installed vertically and the superconducting armature is immersed in a cryostat filled with liquid nitrogen (77 K). The permanent magnet rotor is at room temperature, driven by an asynchronous motor powered by a variable frequency-controlled inverter.

#### 4. Numerical modeling

The experimental characterization by electrical methods as described above allows only to measure global quantities (U, I) which are further used to determine local quantities (E, J) with the assumption of the uniformity of the distribution of both E and J. However, the local quantities can vary significantly due to the strong dependency of the critical current density ( $J_c$ ) to the magnetic field (B). Modeling is thus necessary, and numerical methods are unavoidable in most cases, due to the complexity of the geometry and the nonlinear behavior of the superconductors. In our works, volume integral methods have proved their efficiency to model such systems which are in multi-conductor configurations characterized by multiscale dimensions, where the air regions are consequent. Indeed, the volume integral methods allow to discretize only the active parts of the system.

The magnetic vector potential (A) and the magnetic field (B) are evaluated by integral equations involving volume and surface current densities [24-26]:

$$\begin{cases} \vec{A}(\vec{r}) = \mu_0 \left\{ \int_{\Omega} \vec{J}(\vec{r}') \cdot G(\vec{r}, \vec{r}') d\Omega + \int_{\Gamma} \vec{k}(\vec{r}') \cdot G(\vec{r}, \vec{r}') d\Gamma \right\} \\ \vec{B}(\vec{r}) = \mu_0 \left\{ \int_{\Omega} \vec{J}(\vec{r}') \wedge \vec{\nabla} G(\vec{r}, \vec{r}') d\Omega + \int_{\Gamma} \vec{k}(\vec{r}') \wedge \vec{\nabla} G(\vec{r}, \vec{r}') d\Gamma \right\} \end{cases} \quad (4)$$

The surface current densities are used to model ferromagnetic materials and permanent magnets [27].

The E(J) relation of the superconductor is modelled by the power law (Eq. 1), and the anisotropic dependency of the critical current density to the magnetic field is modeled by the relation (5), where  $J_{c0}$  is the zero field critical current density, and  $k$ ,  $\beta$  and  $B_0$  are parameters depending on the considered HTS [24-27].

$$J_c(B_{\parallel}, B_{\perp}) = \frac{J_{c0}}{\left( 1 + \frac{\sqrt{k^2 B_{\parallel}^2 + B_{\perp}^2}}{B_0} \right)^{\beta}} \quad (5)$$

#### 5. Results and discussions

The U(I) curves measured in the HTS coils inside the machine is presented in figure 5. With a global criterion, the critical current density is reduced to 33A, while it is about 70A for the tape constituting the coils. Using a local criterion (max E), the critical current density drops to about 27A (obtained by simulations). A relatively large gap is obtained between the values of the critical current obtained by the local and global criteria.

The no load voltage obtained in a coil (phase) is shown in Figure 6. The large airgap filters space harmonics providing a quasi-sinusoidal voltage, despite the structure of the machine.

The static torque measured and calculated versus the mechanical rotor position is shown in Figure 7, for an applied current  $I = 25A$  ( $I_a = I$  et  $I_b = I_c = -I/2$ ), and for two values of the airgap (10 & 15mm). The discrepancies between the measurement and the calculation are essentially linked to the uncertainties in the measurements of the air gap and the angle of rotation of the rotor, to the resistive torque generated by the ball bearings placed close to the cryostat,

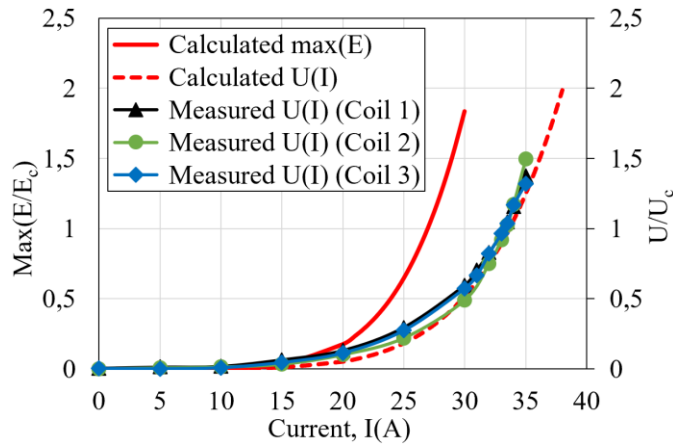


Figure 5. Measured and calculated U(I) curves of HTS coils

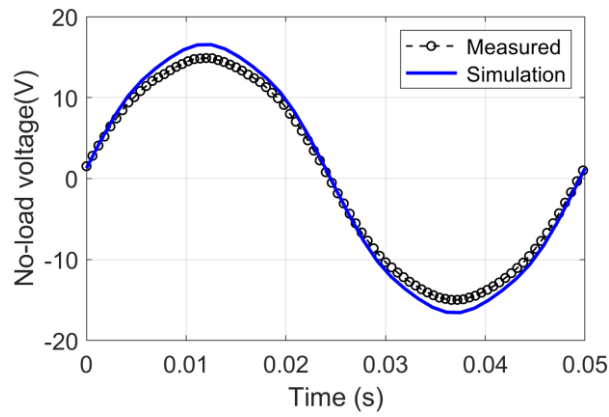


Figure 6. Voltage waveform for a rotational speed of 600 rpm

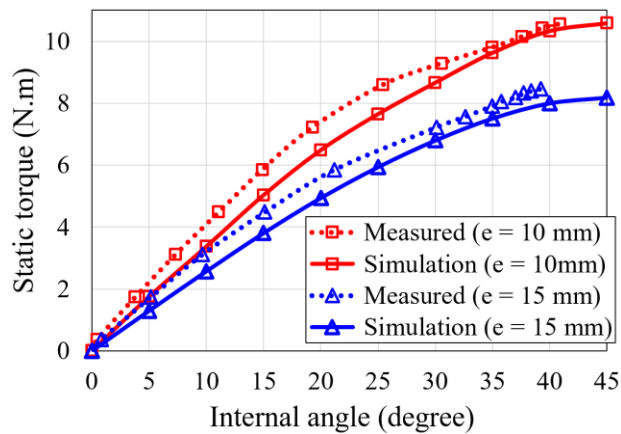


Figure 7. Static torque versus mechanical rotor position,  $I = 25A$  ( $I_a = I$  et  $I_b = I_c = -I/2$ )

## 6. Conclusion

In this work, we presented the experimental tests carried out on a laboratory scale prototype of an axial flux synchronous machine with a superconducting armature.

The prototype and the different measurement methods are described, as well as the integral modeling approach used to calculate the magnetic field produced by all the parts of the prototype. The knowledge of the magnetic field distribution enabled us to determine the critical current of the superconducting coils HTC and also to evaluate the various global quantities characterizing the machine. The experimental results obtained confirm those resulting from the calculation. The obtained results are promising.

During this experimental work, we were confronted with various difficulties linked mainly to the use of superconductors (mechanical stresses, cryogenics, etc.) and to the characterization of AC losses at the machine scale.

## Bibliography

- [1] K. S. Haran et al., "High power density superconducting machines – development status and technology roadmap," *Supercond. Sci. Technol.*, vol. 30, no. 12, pp. 1-30, 2017.
- [2] W. Nick, M. Frank, G. Klaus, J. Fraunhofer, et H.-W. Neumuller, "Operational experience with the world's first 3600 rpm 4 MVA generator at Siemens," *IEEE Trans. Appl. Supercond.*, vol. 17, n° 2, p. 2030–2033, 2007.
- [3] B. Gamble, G. Snitchler, et T. MacDonald, "Full Power Test of a 36.5 MW HTS Propulsion Motor," *IEEE Trans. Appl. Supercond.*, vol. 21, n° 3, p. 1083-1088, juin 2011.
- [4] R. MOULIN, « Dimensionnements et essais de moteurs supraconducteurs », Génie Electrique, université Henri Poincaré, Nancy-I, 2010.
- [5] X. Song et al., « Experimental Validation of a Full-Size Pole Pair Set-Up of an MW-Class Direct Drive Superconducting Wind Turbine Generator », *IEEE Trans. Ener. Conv.*, vol. 35, no. 2, pp. 1120-1128, 2020.
- [6] X. Song et al., « Ground Testing of the World's First MW-Class Direct-Drive Superconducting Wind Turbine Generator », in *IEEE Transactions on Energy Conversion*, vol. 35, no. 2, pp. 757-764, June 2020.
- [7] X. Song et al., « Commissioning of the World's First Full-Scale MW-Class Superconducting Generator on a Direct Drive Wind Turbine », *IEEE Trans. Ener. Conv.*, vol. 35, no. 3, pp. 1697-1704, 2020.
- [8] W. Xian, Y. Yan, W. Yuan, R. Pei, et T. A. Coombs, « Pulsed field magnetization of a high temperature superconducting motor », *IEEE Trans. Appl. Supercond.*, vol. 21, n° 3, p. 1171–1174, 2011.
- [9] P. MASSON, « Étude d'écrans supraconducteurs à haute température critique massifs. Application à la réalisation d'une machine électrique de conception originale », Génie Electrique, Université Henri Poincaré, Nancy I, 2002.
- [10] E. H. Ailam, « Machine synchrone à plots supraconducteurs: Etude et réalisation », *Thèse, Génie Electrique*, Henri Poincaré, Nancy-I, 2006.
- [11] A. Colle, « Etude d'une machine supraconductrice à flux axial pour une application aéronautique », *Thèse, Génie Electrique*, Université de Lorraine, 2020.
- [12] R. Alhasan, « Etude et réalisation d'une nouvelle structure d'un moteur synchrone supraconducteur », *Thèse, Génie Electrique*, Université de Lorraine, 2015.
- [13] D. Sekiguchi et al., « Trial Test of Fully HTS Induction/Synchronous Machine for Next Generation Electric Vehicle », *IEEE Trans. Appl. Supercond.*, vol. 22, no. 3, pp. 5200904-5200904, 2012.
- [14] K Kovalev et al. « Development and testing of 10 kW fully HTS generator », *J. Phys.: Conf. Ser.*, vol. 1559, 2020.
- [15] H. Sugimoto et al., « Development of an Axial Flux Type PM Synchronous Motor With the Liquid Nitrogen Cooled HTS Armature Windings », *IEEE Trans. Appl. Supercond.*, vol. 17, no. 2, pp. 1637-1640, 2007.
- [16] P. Song et al., « Loss measurement and analysis for the prototype generator with HTS stator and permanent magnet rotor », *Physica C: Supercond.*, vol. 494, pp. 225-229, 2013.
- [17] T. Qu et al., « Development and testing of a 2.5 kW synchronous generator with a high temperature superconducting stator and permanent magnet rotor », *Supercond. Sci. Technol.*, vol. 27, 2014.
- [18] G. Messina, E. Tamburo De Bella and L. Morici, « HTS Axial Flux Permanent Magnets Electrical Machine Prototype: Design and Test Results », *IEEE Trans. Appl. Supercond.*, vol. 29, no. 5, pp. 1-5, 2019.
- [19] Francesco Grilli, Anna Kario, « How filaments can reduce AC losses in HTS coated conductors: a review », *Supercond. Sci. Technol.*, vol. 29, pp. 083002, 2016.

- [20] L. Belguerras, « Etudes Théoriques et Expérimentales d'Accouplements Magnétiques Supraconducteurs », Thèse de doctorat, Université de Lorraine, mai 2014.
- [21] B. Dolisy, « Étude d'un moteur supraconducteur à flux axial avec une transmission magnétique supraconductrice intégrée », Thèse, *Génie Electrique*, Université de Lorraine, 2015.
- [22] Y. Statra, H. Menana, B. Douine, T. Lubin, "Axial-Field Synchronous Machine With HTS Armature Windings: Realization and Preliminary Tests", *IEEE Transactions on Applied Superconductivity*, Vol. 32, no. 4, 5200405, 2022.
- [23] Y. Statra, S. Fawaz, H. Menana, B. Douine, "Experimental Electromagnetic Characterization of High Temperature Superconductors Coils Located in Proximity to Electromagnetically Active Materials", *Fluid Dynamic and Material Process* 18 (5), pp. 1529-1537, 2022.
- [24] Y. Statra, H. Menana, L. Belguerras and B. Douine, "A volume integral approach for the modelling and design of HTS coils," *COMPEL*, vol. 38, no. 4, pp. 1133-1140, July 2019.
- [25] Y. Statra, H. Menana, B. Douine, "3D semi-analytical modeling and optimization of fully HTS ironless axial flux electrical machines," *Physica C: Superconductivity and its Applications*, 574, 1353660, 2020.
- [26] S. Fawaz, H. Menana, B. Douine and L. Queval, "DC modeling and characterization of HTS coils with non uniform current density distribution," *Supercond. Sci. Technol.*, 2021.
- [27] Y. Statra, H. Menana, B. Douine, "Semianalytical modeling of AC losses in HTS stacks near ferromagnetic parts", *IEEE Transactions on Applied Superconductivity*, Vol. 31, no.1, 2020.